

## ON NON-SMOOTHNESS IN OPTIMAL DESIGN OF SOLID, ELASTIC PLATES

KENG-TUNG CHENG†

Department of Solid Mechanics, The Technical University of Denmark, Lyngby, Denmark

(Received 22 July 1980; in revised form 27 October 1980)

**Abstract**—In the present paper, minimum compliance design problems of thin, solid elastic plates are discussed. We follow up indications provided by numerical results obtained in a recent paper[1], and propose a new plate model, where a uniform plate is equipped with an infinite number of infinitely thin integral stiffeners. On the basis of this new plate model, numerical and analytical investigations of a new formulation of the minimum compliance design problem are carried out. It is demonstrated that the new formulation is, under certain conditions, superior to the corresponding traditional formulation for determining a possible global optimal solution for solid plates.

Since both the new formulation and the traditional formulation are based on classical thin plate theory, the superiority of the new plate model over the corresponding smooth one directly implies that optimal thickness distributions for thin, solid, elastic plates, are generally not smooth functions, but functions with an infinite number of discontinuities.

### 1. INTRODUCTION

In a recent paper[1] by Olhoff and the author a series of numerical results for minimum compliance design problems of thin, solid elastic plates with given material volume and constraints on the thickness variation are presented. Both results for annular and rectangular plates show a clear tendency of an optimal design with integral stiffeners. The optimal thickness distributions for annular plates further indicate that under some conditions the global optimal design may be a plate, which, at least in some subregions, is equipped with an infinite number of infinitely thin stiffeners.

However, the numerical investigations in [1] cannot be used to follow the whole limiting process and confirm the above conclusion. One obvious reason is that it is impossible to use an infinite number of elements in the numerical computations such as to obtain compliances for plates with an infinite number of discontinuities. Moreover, using finite, but high numbers of elements in the calculations, the results would be encumbered with inevitable numerical errors as more and more thickness jumps emerge in the design. It follows from considerations of this kind that it would be worthwhile to study the possible limiting case directly, i.e. densely stiffened plates, by reformulating the optimal design problem, and to see whether densely stiffened plates are superior to smooth plates or not.

The present paper deals with the problem of minimizing the compliance of thin, solid elastic plates. Unlike the traditional formulation, see, e.g. [7], which usually leads to smooth designs, we in the present paper develop a new plate model in which the thickness is allowed to have an infinite number of discontinuities. Moreover, the density of infinitely thin integral plate stiffeners is used as the design variable in the formulation for optimal design. In order to be consistent with earlier investigations, we still use the Kirchhoff thin plate theory, but take discontinuities of the plate thickness into consideration for deriving the appropriate bending rigidity moduli of the new plate which is, in fact, an anisotropic plate.

Having studied the new plate model, we reformulate the minimum compliance design problem and investigate it both numerically and analytically. On the basis of the complementary energy principle, we obtain certain conditions under which the new plate model is superior to the corresponding smooth one. This superiority is demonstrated by a series of numerical examples for annular plates. By choosing the directions of the stiffeners and varying the thickness of the integrally stiffened plate, we are able to show that the new plate model is

†Visiting from the Department of Solid Mechanics, The Dalian Engineering Institute, Dalian, The People's Republic of China.

indeed superior under quite general conditions. Since the new plate model is formulated on the basis of thin plate theory, which also constitutes the basis for the traditional formulation of optimal design of thin, solid, elastic plates, the superiority directly implies that, in general, the optimal thickness distribution of thin, solid, elastic plates is hardly a smooth function, but a function with an infinite number of discontinuities.

For simplicity, in Section 2, we deal only with annular plates, whose thickness distributions and boundary conditions are axially symmetric. As is in [1], the applied loads are assumed to vary harmonically in the circumferential direction. In Section 3, our study is then extended to solid plates with an arbitrary contour.

## 2. ANNULAR PLATES

### 2(a) Formulation for smooth plates [1, 7]

In polar coordinates,  $r, \theta$ , if we only consider load distribution functions  $p(r, \theta)$  of the special type

$$p(r, \theta) = f(r) \cos n\theta \quad (1)$$

where  $n$  is a given integer, for an annular plate with axisymmetric thickness distribution and boundary conditions, the minimum compliance design problem associated with given material volume and prescribed constraints for the thicknesses  $h(r)$  can be formulated as follows, with  $h(r)$  as the design variable,

$$\begin{aligned} \text{minimize } \Phi &= \int_{\Omega} f(r)w(r)r \, dr \\ \text{subject to } \int_{\Omega} h(r)r \, dr &= 1 \end{aligned} \quad (2)$$

and

$$h_{\min} \leq h \leq h_{\max}, \quad r \in \Omega \{r | R_i \leq r \leq 1\}.$$

Here,  $w(r)$  is the  $\theta$ -independent factorial of the deflection  $W(r, \theta) = w(r) \cos n\theta$  of the plate under the given load  $p(r, \theta)$ , eqn (1), and specific boundary conditions. All variables are dimensionless, and the inner and outer plate radii are  $R_i$  and 1, respectively.

On the basis of the energy principle of linear elasticity, the compliance  $\Phi$  above can also be expressed in terms of the specific strain energy  $\Phi_A$  or complementary energy  $\Phi_C$ , i.e.

$$\Phi = \int_{\Omega} \Phi_A r \, dr = \int_{\Omega} D[\kappa_r^2 + \kappa_{\theta\theta}^2 + 2\nu\kappa_r\kappa_{\theta\theta} + 2(1-\nu)\kappa_{r\theta}^2]r \, dr \quad (3)$$

or

$$\Phi = \int_{\Omega} \Phi_C r \, dr = \int_{\Omega} \frac{1}{D(1-\nu^2)} [M_r^2 + M_{\theta\theta}^2 - 2\nu M_r M_{\theta\theta} + 2(1+\nu)M_{r\theta}^2]r \, dr. \quad (4)$$

Here,

$$D = h^3 \quad (5)$$

and  $\nu$  is Poisson's ratio,  $\kappa_r, \kappa_{\theta\theta}, \kappa_{r\theta}$  are the  $\theta$ -independent factorials of radial, circumferential and twisting curvatures, respectively and  $M_r, M_{\theta\theta}$  and  $M_{r\theta}$  are the  $\theta$ -independent factorials of corresponding moments. The curvature-deflection and moment-curvature relations are given by

$$\kappa_r = w'', \quad \kappa_{\theta\theta} = \frac{w'}{r} - \frac{n^2 w}{r^2}, \quad \kappa_{r\theta} = - \left[ \frac{nw}{r} \right]', \quad (6)$$

and

$$M_r = -D(\kappa_r + \nu\kappa_{\theta\theta}), \quad M_{\theta\theta} = -D(\kappa_{\theta\theta} + \nu\kappa_r), \quad M_{r\theta} = -D(1-\nu)\kappa_{r\theta}, \quad (7)$$

respectively, where primes denote differentiation with respect to  $r$ .

The necessary condition for optimality, which can be derived in different ways [1, 7] is as

follows,

$$\frac{\partial D}{\partial h} [\kappa_{rr}^2 + \kappa_{\theta\theta}^2 + 2\nu\kappa_{rr}\kappa_{\theta\theta} + 2(1 - \nu)\kappa_{r\theta}^2] = \Lambda - \alpha + \beta \tag{8}$$

or

$$\frac{1}{D^2} \frac{\partial D}{\partial h} [M_{rr}^2 + M_{\theta\theta}^2 - 2\nu M_{rr}M_{\theta\theta} + 2(1 + \nu)M_{r\theta}^2] = \Lambda^* - \alpha^* + \beta^*, \tag{9}$$

where  $\Lambda$  and  $\Lambda^*$  are constants, and  $\alpha, \alpha^*, \beta, \beta^*$  are equal to zero at all points  $r$  where the thickness constraints are inactive [1].

2(b) *New plate model*

The numerical results in [1] clearly show the tendency that the optimal design under some conditions may be a plate, which, at least in some of its subregions, is stiffened with infinitely thin stiffeners. Motivated by this indication, a new plate model is proposed here.

The new plate model consists of a uniform part of thickness  $h_{min}$  to which an infinite number of integral stiffeners in the circumferential direction are attached, see Fig. 1. The stiffeners have rectangular cross-sections of fixed height  $(h_{max} - h_{min})$  and infinitesimal width. We further assume that all the stiffeners are placed symmetrically with respect to the mid-plane of the plate. As the design variable, we will choose the density  $b(r)$  of stiffeners defined by

$$b(r) = \lim_{\Delta r \rightarrow 0} \frac{\sum \Delta d_i}{\Delta r} = 1 - \lim_{\Delta r \rightarrow 0} \frac{\sum \Delta c_i}{\Delta r}, \tag{10}$$

where  $\Delta d_i$  is the width of the  $i$ th stiffener,  $\Delta c_i$  is the distance between the  $i$ th stiffener and the  $(i + 1)$ st stiffener. All  $\Delta d_i, \Delta c_i$  and  $\Delta r$  shown in Fig. 1 are infinitesimal.

2(c) *Specific strain energy for the new model*

The total strain energy in the small region  $\Delta r$  can be calculated as a sum of all small contributions. As in [1], all the stiffeners will be assumed to be parts of the plate. Thus, the contribution from the  $i$ th stiffener is

$$\Delta \Phi_i = D_{max} [\kappa_{rr,i}^2 + \kappa_{\theta\theta,i}^2 + 2\nu\kappa_{rr,i}\kappa_{\theta\theta,i} + 2(1 - \nu)\kappa_{r\theta,i}^2] \Delta d_i r_i \tag{11}$$

and the contribution from the  $i$ th small section between the  $i$ th and  $(i + 1)$ st stiffener is

$$\Delta \Phi_r = D_{min} [\kappa_{rr,r}^2 + \kappa_{\theta\theta,r}^2 + 2\nu\kappa_{rr,r}\kappa_{\theta\theta,r} + 2(1 - \nu)\kappa_{r\theta,r}^2] \Delta c_i \bar{r}_i, \tag{12}$$

where

$$D_{max} = h_{max}^3, \quad D_{min} = h_{min}^3. \tag{13}$$

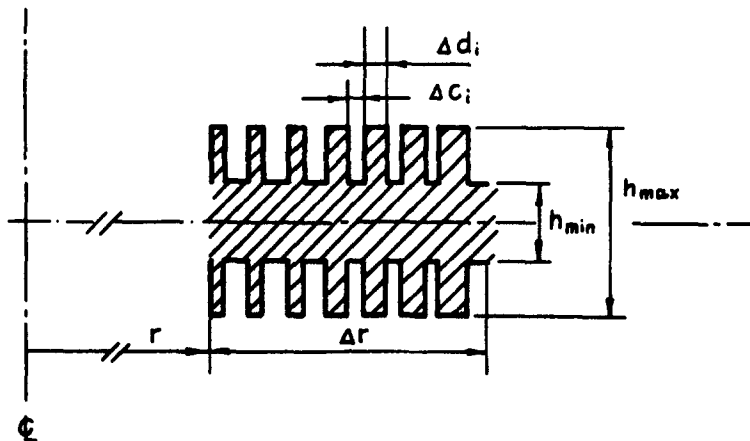


Fig. 1. New plate model.

According to its definition, the specific strain energy is a limit of the average strain energy, i.e.

$$\Phi_A = \lim_{\Delta r \rightarrow 0} \frac{\sum \Delta \Phi_i + \sum \Delta \Phi_r}{\sum \Delta d_i r_i + \sum \Delta c_i r_i} \tag{14}$$

Based on the expressions (11) and (12), the limiting process indicated above cannot be performed because the thickness jumps cause discontinuities in the radial curvature  $\kappa_{rr}$ . In fact, the continuity conditions at interfaces between adjacent subregions only provide continuity of deflection  $w$ , rotation  $w'$ , radial moment  $M_{rr}$  and radial shear force  $Q_r$ . Taking eqn (6) into consideration, curvatures  $\kappa_{\theta\theta}$  and  $\kappa_{r\theta}$  are also continuous. Therefore, alternative expressions  $\Delta \Phi_i$  and  $\Delta \Phi_r$  in terms of continuous quantities can be written as

$$\Delta \Phi_i = \left[ D_{\max}(1 - \nu^2)\kappa_{\theta\theta,i}^2 + 2D_{\max}(1 - \nu)\kappa_{r\theta,i}^2 + \frac{M_{rr,i}^2}{D_{\max}} \right] \Delta d_i r_i \tag{15}$$

$$\Delta \Phi_r = \left[ D_{\min}(1 - \nu^2)\kappa_{\theta\theta,r}^2 + 2D_{\min}(1 - \nu)\kappa_{r\theta,r}^2 + \frac{M_{rr,r}^2}{D_{\min}} \right] \Delta c_i r_i \tag{16}$$

Substituting them into eqn (14) and completing the limiting process, we obtain

$$\Phi_A = [D_{\min} + b(r)(D_{\max} - D_{\min})][(1 - \nu^2)\kappa_{\theta\theta}^2 + 2(1 - \nu)\kappa_{r\theta}^2] + M_{rr}^2 \left[ \frac{b(r)}{D_{\max}} + \frac{1 - b(r)}{D_{\min}} \right] \tag{17}$$

The radial curvature  $\kappa_{rr}$  for plates is, in general, defined as

$$\kappa_{rr} = \frac{d^2 w}{dr^2} = \lim_{\Delta r \rightarrow 0} \left[ \frac{dw}{dr} \Big|_{r+\Delta r} - \frac{dw}{dr} \Big|_r \right] / \Delta r \tag{18}$$

Then, the radial curvature  $\kappa_{rr}$  for the new plate model can be expressed as

$$\kappa_{rr} = \lim_{\Delta r \rightarrow 0} \frac{\sum \kappa_{rr,i} \Delta d_i + \sum \kappa_{rr,r} \Delta c_i}{\Delta r} \tag{19}$$

Expressing  $\kappa_{rr,i}$  and  $\kappa_{rr,r}$  by means of  $M_{rr,i}$ ,  $\kappa_{\theta\theta,i}$ , ..., and substituting into (19), the continuity of  $M_{rr}$  and  $\kappa_{\theta\theta}$  leads to

$$M_{rr} = \left[ \frac{b(r)}{D_{\max}} + \frac{1 - b(r)}{D_{\min}} \right]^{-1} (\kappa_{rr} + \nu \kappa_{\theta\theta}) \tag{20}$$

Resubstituting (20) into (17), we have the specific strain energy

$$\begin{aligned} \Phi_A = & [D_{\min} + b(D_{\max} - D_{\min})][\kappa_{rr}^2 + \kappa_{\theta\theta}^2 + 2\nu\kappa_{rr}\kappa_{\theta\theta} + 2(1 - \nu)\kappa_{r\theta}^2] \\ & + b(b - 1)(\kappa_{rr} + \nu\kappa_{\theta\theta})^2 (D_{\max} - D_{\min})^2 [bD_{\min} + (1 - b)D_{\max}] \end{aligned} \tag{21}$$

Finally, we emphasize that the above derivation is completely consistent with the classical plate theory, which also constitutes the basis for the traditional formulation of optimal design of thin, solid, elastic plates. Therefore, a solution of this new model provides a limiting solution of a series of solid plates, whose numbers of thickness discontinuities tend to infinity. However, from a practical point of view, the new model has some shortcomings. For example, the very thin stiffeners may buckle, and the classical assumption concerning straight normals is hardly valid when the thickness of the plate undergoes sharp variations. The traditional formulation for optimal design of thin, solid, elastic plates is, however, also subject to these shortcomings, but since it is our objective here to study the results of optimizing solid plates, with the usual assumptions included in the theory, we disregard possible shortcomings of this theory.

2(d) *Minimum compliance design formulation for the new plate model*

Having obtained the specific strain energy, it is straightforward to derive the moment-curvature relations for the new model. After introducing the convenient short-hand notation

$$D_r = \frac{D_{\max} D_{\min}}{b D_{\min} + (1-b) D_{\max}}, \quad D_{r\theta} = b D_{\max} + (1-b) D_{\min}$$

and

$$D_\theta = (1-\nu^2) D_{r\theta} + \nu^2 D_r, \quad \nu_r = \frac{D_r \nu}{D_\theta}, \quad (22)$$

the moment-curvature relations can be written as

$$M_{rr} = -D_r (\kappa_{rr} + \nu \kappa_{\theta\theta}), \quad M_{\theta\theta} = -D_\theta (\kappa_{\theta\theta} + \nu_r \kappa_{rr}), \quad M_{r\theta} = -D_{r\theta} (1-\nu) \kappa_{r\theta}, \quad (23)$$

or

$$\kappa_{rr} = \frac{-\nu (M_{rr} - \nu_r M_{\theta\theta})}{\nu_r D_{r\theta} (1-\nu^2)}, \quad \kappa_{\theta\theta} = \frac{-(M_{\theta\theta} - \nu M_{rr})}{D_{r\theta} (1-\nu^2)}, \quad \kappa_{r\theta} = \frac{-M_{r\theta}}{D_{r\theta} (1-\nu)}. \quad (24)$$

In the above manipulations the following identity

$$D_{r\theta} = D_r \left[ 1 + \frac{b(1-b)(D_{\max} - D_{\min})^2}{D_{\max} D_{\min}} \right] \quad (25)$$

has frequently been used.

By studying the moment-curvature relations, it is noticed that the new model is nothing but a plate made of cylindrical anisotropic material[4], for which the governing equations are available in [4, 5].

For the linearly elastic materials considered here the specific complementary energy  $\Phi_c$  is easily obtained if we substitute (24) into (21),

$$\Phi_c = \frac{1}{D_{r\theta} (1-\nu^2)} [M_{rr}^2 - 2\nu M_{rr} M_{\theta\theta} + M_{\theta\theta}^2 + 2(1+\nu) M_{r\theta}^2] + \frac{D_{r\theta} - D_r}{D_r D_{r\theta}} M_{rr}^2. \quad (26)$$

Let us now formulate the minimum compliance design problem for the new plate model as follows:

With  $b(r)$  as the design variable, minimize  $\Phi = \int_\Omega f(r) w(r) r \, dr$  subject to the volume constraint

$$\int_\Omega [b h_{\max} + (1-b) h_{\min}] r \, dr = 1 \quad (27a)$$

and the density constraints

$$0 \leq b(r) \leq 1. \quad (27b)$$

Again,  $w(r)$  is the  $\theta$ -independent factorial of deflection of the plate under given load  $p(r, \theta) = f(r) \cos n\theta$  and certain boundary conditions.

Applying the Lagrange multiplier method[1], the necessary condition for optimality is found to be

$$(D_{\max} - D_{\min}) [(1-\nu^2) \kappa_{\theta\theta}^2 + 2(1-\nu) \kappa_{r\theta}^2] - M_{rr}^2 \left[ \frac{1}{D_{\max}} - \frac{1}{D_{\min}} \right] = \Lambda (h_{\max} - h_{\min}) - \alpha + \beta, \quad (28)$$

where  $\Lambda$  is a constant and  $\alpha$  and  $\beta$  satisfy

$$\begin{aligned} \alpha = 0, \quad \beta = 0 & \text{ when } 0 < b(r) < 1, \\ \alpha \neq 0, \quad \beta = 0 & \text{ when } b(r) = 0, \\ \alpha = 0, \quad \beta \neq 0 & \text{ when } b(r) = 1. \end{aligned}$$

Several numerical solutions are presented in Section 2(g).

2(e) *Min-min problems.*

In order to make a theoretical comparison between solid plates and corresponding new model plates, let us cast the above formulations (2), (27) into min-min problems[2]. This is mainly done on the basis of the minimum complementary energy principle, which can be stated as[3]:

For the statically admissible moment field associated with an actual displacement field, the total complementary energy attains a minimum value when compared to values resulting from any other statically admissible moment field.

As is well known, the compliance of a structure of linear elastic material equals the total complementary energy of the structure, when it is in equilibrium. Therefore, the minimum compliance design problem can easily be reformulated as a min-min problem [2], i.e.

$$\text{Min}_{\text{admissible designs}} \left\{ \text{Min}_{\text{admissible moments}} \left\{ \int_{\Omega} \Phi_c r \, dr \right\} \right\}. \tag{29}$$

The expressions for  $\Phi_c$  of solid plates and new plates are given in (4) and (26), respectively. The so-called admissible designs are conceived as designs which satisfy the given constraints for the volume and for the design variable. The admissible moment field is to satisfy the statical boundary conditions and equilibrium equations in terms of moments. For both solid plates and new model plates, the set of admissible moment fields will be completely the same if the same loads and statical boundary conditions are considered. In other words, a statically admissible moment field for a solid plate is also an admissible one for the new model plate and vice versa, if they have the same  $R_i$ , applied loads and statical boundary conditions. Furthermore, keeping the statical boundary conditions and external loads unchanged, the actual moment field for a solid plate is certainly an admissible moment field for the new model plate.

2(f) *Superiority of the new model*

The following theorem establishes the conditions under which a new model plate is superior to the corresponding smooth one.

*Theorem A.* Suppose that there in a smooth, solid plate optimal design exists a subregion  $\Omega_s \{r|a \leq r \leq d\}$  where  $h_{\min} < h < h_{\max}$  and where the actual moments satisfy

$$\frac{M_{rr}^2}{[M_{rr}^2 - 2\nu M_{rr} M_{\theta\theta} + M_{\theta\theta}^2 + 2(1 + \nu)M_{r\theta}^2]} < \frac{(\alpha + \beta + 1)\beta^3}{(1 - \nu^2)(\beta^2 + \beta + 1)^2\alpha^3} \tag{30}$$

with  $\alpha = h/h_{\min}$  and  $\beta = h_{\max}/h_{\min}$ . Then, the compliance will be further decreased if the material distribution is kept unchanged, but a new model section is constructed instead of the original one in  $\Omega_s$ .

*Proof.* Let  $\Phi^s$  denote the compliance of the original smooth design. By means of its actual moments  $M_{rr}$ ,  $M_{\theta\theta}$  and  $M_{r\theta}$ , eqn (4) leads to

$$\Phi^s = \int_{\Omega} \frac{1}{D(1 - \nu^2)} [M_{rr}^2 - 2\nu M_{rr} M_{\theta\theta} + M_{\theta\theta}^2 + 2(1 + \nu)M_{r\theta}^2] r \, dr. \tag{31}$$

Now we change the smooth plate section into the new model section and obtain a new plate.

During that change, the material distribution is kept unchanged, i.e. the density  $b(r)$  of stiffeners in  $\Omega$ , satisfies

$$h_{\min} + b(r)(h_{\max} - h_{\min}) = h(r)$$

and

$$r \in \Omega, \quad (32)$$

$$0 < b(r) < 1.$$

Taking the moments  $M_{rr}$ ,  $M_{\theta\theta}$  and  $M_{r\theta}$  as statically admissible ones for the new plate, the integral in eqn (29) can be calculated as

$$\begin{aligned} \Phi^A = & \int_{\Omega_1} \left\{ \frac{1}{D_{r\theta}(1-\nu^2)} [M_{rr}^2 - 2\nu M_{rr}M_{\theta\theta} + M_{\theta\theta}^2 + 2(1+\nu)M_{r\theta}^2] \right. \\ & \left. + \frac{D_{r\theta} - D_r}{D_r D_{r\theta}} M_{r\theta}^2 \right\} r \, dr \end{aligned} \quad (33)$$

$$+ \int_{\Omega_1} \frac{1}{D(1-\nu^2)} [M_{rr}^2 - 2\nu M_{rr}M_{\theta\theta} + M_{\theta\theta}^2 + 2(1+\nu)M_{r\theta}^2] r \, dr,$$

where

$$\Omega_1 = \Omega - \Omega_s. \quad (34)$$

According to (29), it turns out that

$$\Phi^N \leq \Phi^A, \quad (35)$$

where  $\Phi^N$  denotes the actual compliance for the new plate. Based on (31) and (33), the difference between  $\Phi^A$  and  $\Phi^s$  is given by

$$\Phi^A - \Phi^s = \int_{\Omega_1} \left\{ \frac{(D_{r\theta}^{-1} - D^{-1})}{(1-\nu^2)} [M_{rr}^2 - 2\nu M_{rr}M_{\theta\theta} + M_{\theta\theta}^2 + 2(1+\nu)M_{r\theta}^2] + (D_r^{-1} - D_{r\theta}^{-1})M_{r\theta}^2 \right\} r \, dr, \quad (36)$$

which will certainly be less than zero if the integrand on the r.h.s. is less than zero everywhere in  $\Omega_1$ . The latter condition is identical with the following inequality,

$$\frac{M_{r\theta}^2}{[M_{rr}^2 - 2\nu M_{rr}M_{\theta\theta} + M_{\theta\theta}^2 + 2(1+\nu)M_{r\theta}^2]} < \frac{1}{1-\nu^2} \left[ \frac{1}{D} - \frac{1}{D_{r\theta}} \right] \frac{D_r D_{r\theta}}{(D_{r\theta} - D_r)}. \quad (37)$$

Solving  $b(r)$  from eqn (32) and inserting it into eqn (22) and (37), some algebraic manipulations furnish

$$\left[ \frac{1}{D} - \frac{1}{D_{r\theta}} \right] \frac{D_r D_{r\theta}}{(D_{r\theta} - D_r)} = \frac{(\alpha + \beta + 1)\beta^3}{(\beta^2 + \beta + 1)^2 \alpha^3}. \quad (38)$$

Comparing (38) with (30), we conclude that if eqn (30) is satisfied everywhere in  $\Omega_s$ , we will have

$$\Phi^A - \Phi^s < 0 \text{ or } \Phi^A < \Phi^s. \quad (39)$$

Taking eqn (35) into consideration, we further come to the conclusion that if the conditions of Theorem A hold, then the inequality

$$\Phi^N < \Phi^s \quad (40)$$

will hold good. However, eqn (40) simply implies superiority of the new model over the original smooth one, i.e. the latter cannot constitute a global optimal solution.

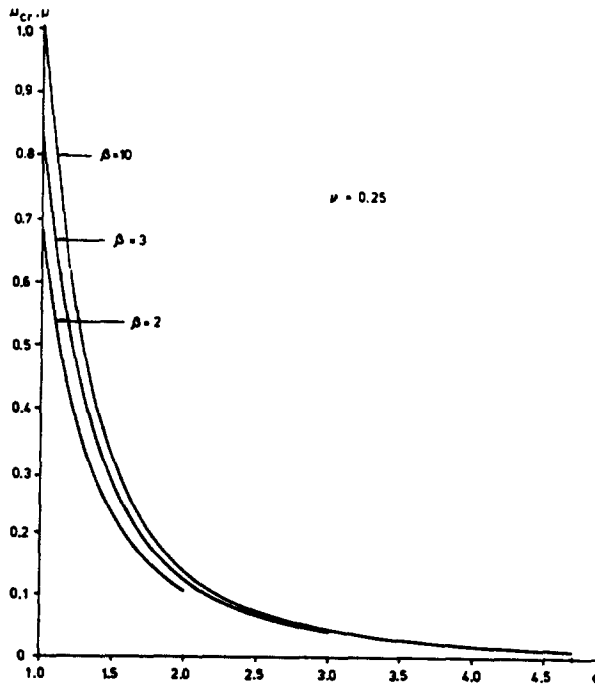


Fig. 2. Below the curves a smooth design can be improved by constructing a new model section.  $\mu$ ,  $\alpha$  are given in (41).  $\mu_{cr}$  is given in (30).

In order to discuss this result, let us denote the expression on the r.h.s. of (30) by  $\mu_{cr}$ . Figure 2 shows  $\mu_{cr}$  by a set of curves vs  $\alpha$  for different  $\beta$ . With a smooth (or partially smooth) local optimal design for a solid plate and its actual moments in hand, the curves in Fig. 2 can serve to determine whether there exists a new model plate that is superior to the smooth one. This can be done as follows. First, using the available thicknesses and moments, we calculate

$$\alpha = \frac{h}{h_{\min}}, \quad \mu = \frac{M_{rr}^2}{[M_{rr}^2 - 2\nu M_{rr}M_{\theta\theta} + M_{\theta\theta}^2 + 2(1 + \nu)M_{r\theta}^2]} \quad (41)$$

at each point of subregions where  $h_{\min} < h < h_{\max}$ . Then points with coordinates  $(\alpha, \mu)$  are plotted in Fig. 2. If some of these points lie below the curve corresponding to the given  $\beta$ , it can be concluded that there exists a new model plate that is better than the smooth one.

Two interesting features should be emphasized here.

1. For any finite  $\beta$ ,  $\beta > 0$ , points with  $M_{rr} = 0$  are always below the curves. This means that along curves with  $M_{rr} = 0$ , it is always worthwhile to construct a new model section instead of the original smooth one, no matter how small  $\beta$  ( $\beta > 0$ ) is.

2. For large values of  $\beta$ , the new model plate can be still better than the corresponding smooth one although  $M_{rr}^2$  is rather large in comparison with

$$M_{rr}^2 - 2\nu M_{rr}M_{\theta\theta} + M_{\theta\theta}^2 + 2(1 + \nu)M_{r\theta}^2,$$

as long as condition (30) holds good. This statement is consistent with the result in [2], where Reiss proved that the compliance can be made arbitrarily small for a simply supported solid circular plate subjected to any axisymmetric loading unless this includes a concentrated load at the plate centre.

Theorem A indicates that a global optimal thickness distribution for a solid plate is probably a mixed structure of smooth thickness segments and new model segments. However, on the basis of Theorem A, the following corollary can be established.



(Corollary 1. If the thickness  $h$  satisfies

$$h_{\min} < h < h_{\max},$$

in any smooth part of a global, optimal, solid plate design, then the actual moments must violate condition (30).

Finally, it should be emphasized that the condition in Theorem A is only a sufficient one. For points lying above the curves in Fig. 2, there still exist the possibility that a new model plate may be superior to the corresponding smooth one.

### 2(g) Example

Since the above results hold for full circular plates as well, we consider in the following an example of a full circular plate with unit radius and uniformly distributed edge moments  $M_0$  applied to the outer edge. For this example, see Ref. [2], a uniform thickness distribution constitutes a local optimal design, as may easily be checked by solving the plate equation and boundary conditions, and then substituting its solutions

$$M_{rr} = M_{\theta\theta} = M_0, \quad w = \frac{M_0}{2h^3(1+\nu)}(1-r^2) \quad (42)$$

into the necessary condition (7) or (8) for optimality. The corresponding compliance

$$\Phi = \frac{M_0^2}{h^3(1+\nu)} \quad (43)$$

is determined as the work done by the edge moments  $M_0$ .

Now let us turn to the new model, i.e. a full circular plate consisting of a uniform part of thickness  $h_{\min}$  to which is attached a set of *uniformly* distributed stiffeners of height  $(h_{\max} - h_{\min})$  and density

$$b(r) = (h - h_{\min}) / (h_{\max} - h_{\min}) = (\alpha - 1) / (\beta - 1),$$

where  $h_{\max}$  and  $h_{\min}$  are all given.

Referring to the theory of anisotropic plates [4, 5], the solution

$$w = \frac{M_0}{D_r(m+\nu)(m+1)}(1-r^{m+1}),$$

$$M_{rr} = M_0 r^{m-1}, \quad M_{\theta\theta} = \frac{M_0 \nu}{(m+\nu)} \left[ m + \frac{1}{\nu_r} \right] r^{m-1} \quad (44)$$

for the new plate enables us to obtain the following compliance

$$\Phi_N = \frac{M_0^2}{D_r(m+\nu)}, \quad (45)$$

where

$$m^2 = \frac{D_\theta}{D_r} = [b + (1-b)\beta^{-3}][b + (1-b)\beta^3](1-\nu^2) + \nu^2. \quad (46)$$

Although the new plate has uniformly distributed stiffeners, which is not an optimal choice for this type of plates, its compliance  $\Phi_N$  is already lower than the corresponding  $\Phi$  in (43) when the conditions in Theorem A hold. The three curves in Fig. 3 show the dependence of  $\Phi/\Phi_N$  on  $h_{\min}$  for different values of  $h_{\max}$ . Notice that the fact that the conditions in Theorem A are only sufficient conditions, is directly implied in Fig. 3.

### 2(h) Numerical results and discussions

The minimum compliance design problems for the new model plates are now solved

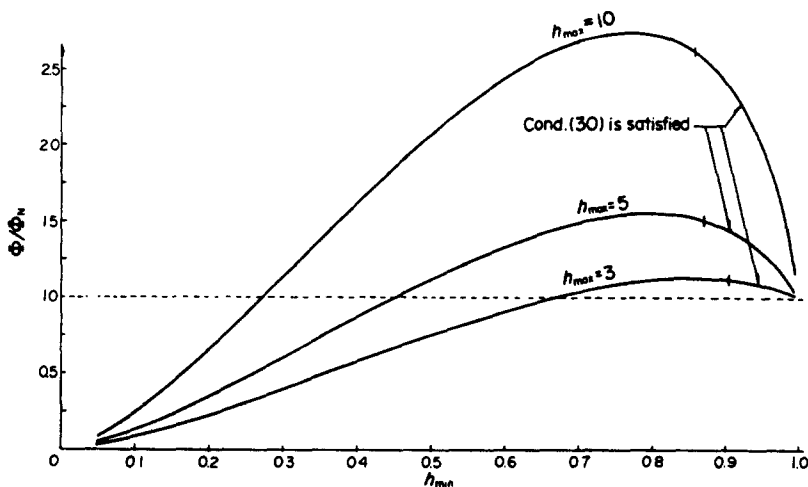


Fig. 3. Compliance comparisons. Full circular plates, uniformly distributed edge moment,  $\Phi$ -compliance of uniform, solid plates,  $\Phi_u$ -compliance of uniform, new plate model.  $h = 1.0$ ,  $\nu = 0.25$ .

numerically. The general iterative scheme developed in [1] is slightly revised and used to obtain all the numerical results presented in the following.

To compare with the numerical results for solid plates in [1], the plate to be optimized below has the same Poisson's ratio  $\nu = 0.25$  and same geometrical size as in [1], i.e. the inner plate radius is taken to be one-fifth of the outer plate radius, the ratio between the thickness constraints is  $h_{\max}/h_{\min} = 5$  and  $h_{\min}$  is given via the ratio  $h_u/h_{\min} = 1.6579$ , where  $h_u$  is the solid plate thickness corresponding to a uniform distribution of the available volume over the plate area. Figure 4(a)–(i) illustrate numerical solutions for annular, new model plates with the nine possible combinations of clamped, simply supported and free inner and outer plate edges. Each solution is illustrated by a radial section through the plate, together with the  $\theta$ -independent part  $w(r)$  of the deflection function. All the results are associated with the load wave number  $n = 4$ , and 50 elements are used in the numerical calculations. In Table 1, we list the corresponding compliances for the nine combinations. As is in [1], we state the compliances as fractions of the compliance  $\Phi_{u,s}$  of a corresponding uniform plate that has the same loading, boundary conditions, total volume and inner and outer plate radii, and that is made of the same material. The results in the second column are the minimum compliances for solid plates quoted from Fig. 5 in [1]. The third column shows compliances for new model plates, which consist of uniform plates of thickness  $h_{\min}$  and uniform density distributions  $b(r)$  of integral stiffeners. Comparisons of the numerical results in the second and third column give a clear demonstration of the superiority of the new model plate. In the last column we show the minimum compliances for the new model plates, which correspond to the optimal designs shown in Fig. 4(a)–(i). Referring to the results in the third column, it is obvious that for the new model plates themselves, we gain very little by the optimization. This may be explained by the fact that the new type of structure, i.e. the new model plate, is itself an optimal one in the present case.

The above results should not lead to the impression that the new model plates are always superior to the corresponding solid ones. Our numerical results reveal that there are situations in which the optimal design for the new model plate is even inferior to the corresponding uniform, solid one. Let us take the clamped–clamped plate as an example, and optimize it subject to the load wave number  $n = 0$ . Results for  $h_{\max}/h_{\min} = 5$  and  $h_{\max}/h_{\min} = 20$  are shown in Figs. 5(a) and (b), respectively. Stating the compliances as a fraction of the compliance  $\Phi_{u,s}$  as before, the compliance for the optimal new model plate is equal to 1.016 for  $h_{\max}/h_{\min} = 5$ , which implies that the optimal new model plate is even inferior to the corresponding uniform, solid one. However, with  $h_{\max}/h_{\min} = 20$ , we find  $\Phi_{m,n}/\Phi_{u,s} = 0.290$ , i.e. the new model plate is certainly superior. It is obvious that the inferiority of the new plate model in the present case is due to the fact that the stiffeners are oriented in a direction in which the moment does not

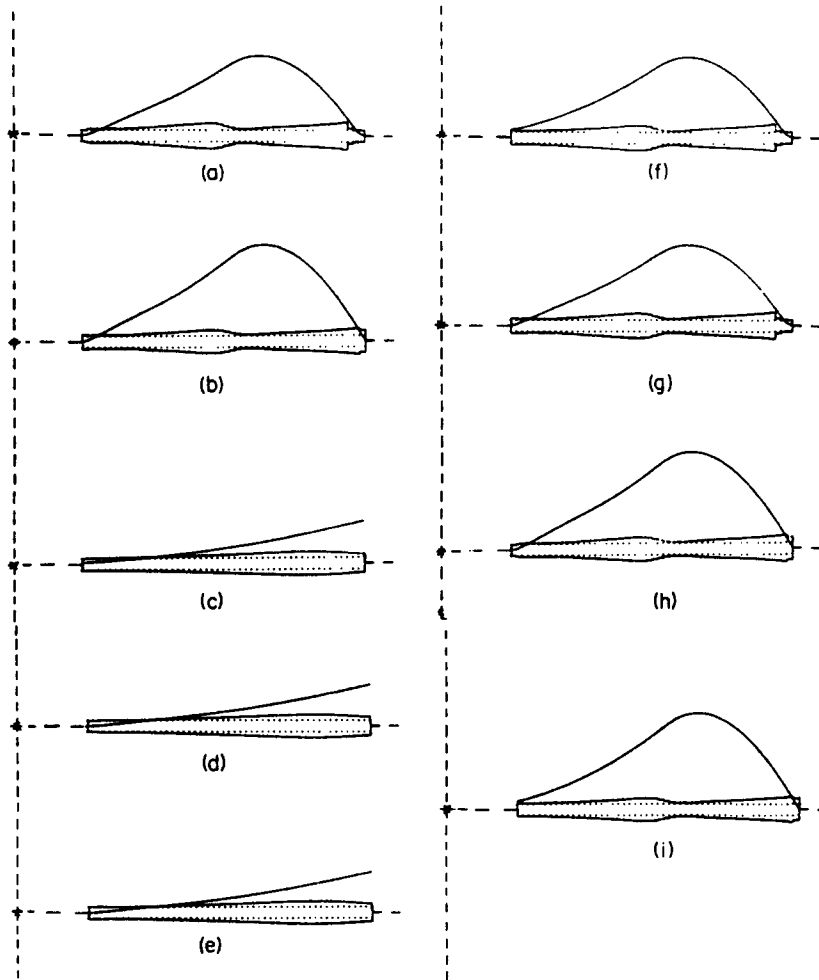


Fig. 4. Results of optimizing annular, new model plates of different boundary conditions. Dotted lines show radial sections of their uniform parts. Densities of stiffeners are visualized by the distances between solid curves and dotted lines. In each picture the  $\theta$ -independent part  $w$  of the deflection function is also indicated by a solid curve. (a) Clamped-clamped plate. (b) Simply supported-simply supported plate. (c) Free-free plate. (d) Clamped-free plate. (e) Simply supported-free plate. (f) Free-clamped plate. (g) Simply supported-clamped plate. (h) Clamped-simply supported plate. (i) Free-simply supported plate,  $n = 4$ , 50 elements. Their compliances are given in Table 1.

Table 1. Comparison between solid plates and new plate models

B. C.	$\phi_{m,s}/\phi_{u,s}$	$\phi_{u,n}/\phi_{u,s}$	$\phi_{m,n}/\phi_{u,s}$
c - c	0.536	0.444	0.415
s - s	0.605	0.324	0.302
f - f	0.265	0.215	0.198
c - f	0.251	0.217	0.198
s - f	0.256	0.215	0.197
f - c	0.617	0.430	0.404
s - c	0.564	0.434	0.407
c - s	0.584	0.330	0.307
f - s	0.645	0.323	0.302

Boundary conditions at inner and outer edges are indicated in the first column. c—clamped, s—simply supported, f—free. Subscripts s, n, m and u refers to solid plates, new model plates, minimum compliance design and uniform design, respectively.

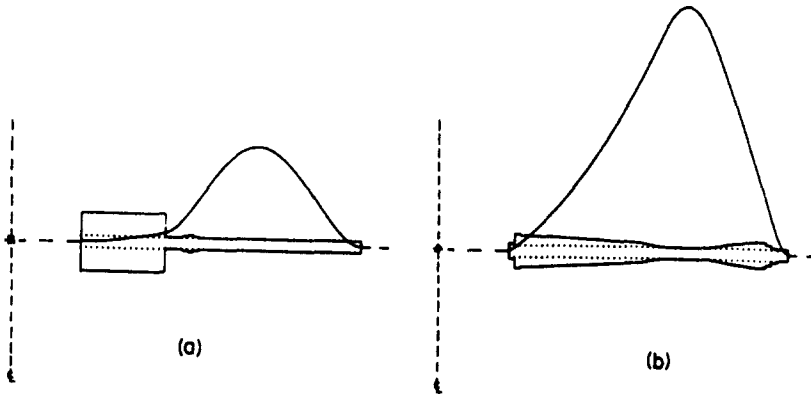


Fig. 5. Influences of ratio  $h_{\max}/h_{\min}$  on the comparisons between new model plates and solid plates. Axisymmetric uniform loads.  $R_1 = 0.2$ . Both inner and outer plate edges are clamped. (a)  $h_{\max}/h_{\min} = 5$ ,  $\Phi_{m,n}/\Phi_{s,n} = 1.016$ . (b)  $h_{\max}/h_{\min} = 20$ ,  $\Phi_{m,n}/\Phi_{s,n} = 0.290$ . The deflection curve in (b) is amplified 10 times.

dominate. It will be shown in Section 3 that by choosing the directions of the stiffeners and varying the thickness of the integrally stiffened plate, the new plate model is, in fact, superior under quite general conditions.

It should finally be mentioned that the new model plates overestimate the stiffness of the physical structure, particularly when the density  $b(r)$  is very small. As is well known, a very thin stiffener should be considered as a thin curved beam whose strains are described by the theory of small deformations of thin curved beams[9].

### 3. A GENERALIZED NEW SOLID PLATE MODEL AND ITS SUPERIORITY

From the above discussion of annular plates one can clearly see the feature of thin, solid, elastic plates: that the compliance can be further decreased by introducing an infinite number of discontinuities into the thickness distribution, while keeping the material distribution unchanged.† It is also discovered in Section 2(h) that the directions of the stiffeners play a crucial role in the superiority of the new plate model. It will be shown in the following that, by choosing the directions of the stiffeners and varying the thickness of the integrally stiffened solid plate, a generalized, integrally stiffened solid plate model will be superior to the corresponding smooth one under quite general conditions.

The generalized, integrally stiffened, solid plate model consists of a smooth part of varying thickness  $h_c(x, y)$ , which is equipped with an infinite number of integral stiffeners in suitable directions. These directions will be determined in the following. We also assume that the stiffeners have rectangular cross-sections of varying height ( $h_{\max} - h_c$ ) and infinitesimal width, and that only one stiffener is allowed at each point of the plate.

Let us consider the vicinity of an arbitrary point  $(x, y)$  of a plate, see Fig. 6, and introduce a local rectangular coordinate system  $(\xi, \eta)$ , in which the  $\xi$  axis coincides with the direction of the stiffeners. On the basis of the derivation given in 2(c) and 2(d), which is not restricted to annular plates, we can immediately write the expression for the specific complementary energy as follows,

$$\Phi_c = \frac{1}{D_{\xi\eta}(1-\nu^2)} [M_{\eta\eta}^2 - 2\nu M_{\xi\xi} M_{\eta\eta} + M_{\xi\xi}^2 + 2(1+\nu)M_{\xi\eta}^2] + \frac{D_{\xi\eta} - D_\eta}{D_\eta D_{\xi\eta}} M_{\eta\eta}^2, \quad (47)$$

†This feature is unique for solid plates. In [11], it is proved that in the case of sandwich plates and "beam stiffened plates" the compliance cannot be reduced by introducing an infinite number of discontinuities into smooth designs while keeping the material distribution unchanged.

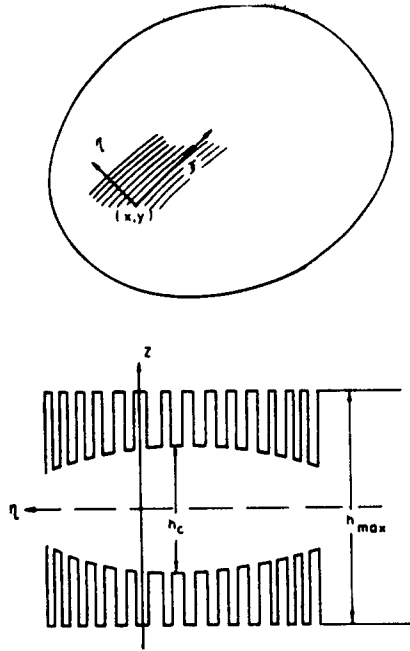


Fig. 6. Generalized new plate model.

where

$$D_\eta = \frac{D_{\max} D_c}{b D_c + (1 - b) D_{\max}}, \quad D_{\xi\eta} = b D_{\max} + (1 - b) D_c \quad (48)$$

$$D_c = h_c^3, \quad (49)$$

and where  $M_{\xi\xi}$  and  $M_{\eta\eta}$  are the bending moments in the  $\xi$  and  $\eta$  directions, respectively, and  $M_{\xi\eta}$  is the twisting moment.

The comparison between smooth plates and the new plates will be performed via the same logic as was used in Section 2. Assume first that we have obtained a smooth (or partially smooth) solid plate, together with its actual moments and compliance  $\Phi^s$ , for given load and boundary conditions. Keeping the material distribution unchanged, it is our aim to change the smooth part into the new model. On the basis of the complementary energy principle, the actual compliance  $\Phi^N$  of the new plate satisfies

$$\Phi^N \leq \Phi^A, \quad (50)$$

where  $\Phi^A$  is obtained by substituting admissible moments into the complementary energy expression. Using the actual moments of the smooth design as admissible moments for the new plate, we obtain

$$\begin{aligned} \Phi^A - \Phi^s = \int_{\Omega} \left\{ \frac{(D_{\xi\eta}^{-1} - D^{-1})}{(1 - \nu^2)} [M_{\eta\eta}^2 - 2\nu M_{\xi\xi} M_{\eta\eta} + M_{\xi\xi}^2 + 2(1 + \nu) M_{\xi\eta}^2] \right. \\ \left. + (D_\eta^{-1} - D_{\xi\eta}^{-1}) M_{\eta\eta}^2 \right\} d\xi d\eta. \end{aligned} \quad (51)$$

In order to have

$$\Phi_A < \Phi^s, \quad (52)$$

we adjust the directions of the stiffeners and the thickness  $h_c$  at each point such that the integrand becomes as large a negative value as possible. At a point where a negative value of

the integrand cannot be achieved, we keep the original smooth design unchanged. Obviously, the subregions of the original smooth design, where  $h = h_{\max}$  or  $h = h_{\min}$ , should not be changed, and we need only consider subregions where

$$h_{\min} < h < h_{\max}.$$

It is always possible to partition such a subregion into two subregions  $\Omega_0$ , and  $\Omega_{\eta}$ , where the two principal moments  $M_1, M_2$  have opposite signs and the same signs, respectively. At any point of  $\Omega_0$ , there will exist an  $\eta$ -direction such that

$$M_{\eta\eta} = 0, \tag{53}$$

since the two principal moments have opposite signs. In subregion  $\Omega_0$ , we now place the stiffeners in the direction perpendicular to the  $\eta$ -direction, i.e. the  $\xi$ -direction, and choose the thickness  $h_c$  as

$$h_c = h_{\min}. \tag{54}$$

By means of these choices, the integrand becomes negative,

$$\frac{(D_{\xi\xi}^{-1} - D^{-1})}{(1 - \nu^2)} [M_{\xi\xi}^2 + 2(1 + \nu)M_{\xi\eta}^2] < 0, \tag{55}$$

because with unchanged material distribution, the density of stiffeners

$$b = (h - h_{\min}) / (h_{\max} - h_{\min}), \tag{56}$$

leads to

$$D_{\xi\eta}^{-1} - D^{-1} = [bD_{\max} + (1 - b)D_{\min}]^{-1} - D^{-1} < 0. \tag{57}$$

Note that inequality (55) does not hold good if  $M_{\xi\xi} = M_{\xi\eta} = 0$ . However, the optimality condition prevents points with  $M_{\xi\xi} = M_{\eta\eta} = M_{\xi\eta} = 0$  from having intermediate thicknesses. Therefore, inequality (55) holds strictly.

Let us now turn to a subregion  $\Omega_{\eta}$ , where the two principal moments  $M_1$  and  $M_2$  satisfy

$$M_1 \cdot M_2 \leq 0. \tag{58}$$

Denoting the smaller of  $|M_1|$  and  $|M_2|$  by  $|M_{\eta\eta}|$ , and placing the stiffeners in the  $\xi$ -direction, the integrand

$$I = \frac{(D_{\xi\xi}^{-1} - D^{-1})}{(1 - \nu^2)} [M_{\eta\eta}^2 - 2\nu M_{\xi\xi} M_{\eta\eta} + M_{\xi\xi}^2] + (D_{\eta}^{-1} - D_{\xi\eta}^{-1}) M_{\eta\eta}^2 \tag{59}$$

can be considered a function of  $h_c$  for a given set of  $M_{\xi\xi}, M_{\eta\eta}, h_{\max}$  and  $h_c$ . We have found that in order to obtain such an  $h_c$  that

$$I < 0, \tag{60}$$

$h$  must satisfy the condition

$$\frac{(1 + 2\alpha)}{(1 - \nu^2)(1 + \alpha + \alpha^2)^2} > \frac{1}{g}, \tag{61}$$

where

$$\alpha = h/h_{\max} \text{ and } g = \frac{M_{\xi\xi}^2 - 2\nu M_{\xi\xi} M_{\eta\eta} + M_{\eta\eta}^2}{M_{\eta\eta}^2} \tag{62}$$

$$\text{and } g = \lambda^2 - 2\nu\lambda + 1, \quad \lambda = \frac{M_{\xi\xi}}{M_{\eta\eta}}.$$

It is noteworthy that condition (61) is precisely the same condition as was proposed by Lurie and Cherkvaev in [10], where they studied the maximum fundamental frequency design problem for thin, solid, elastic plates, and considered the effect of strong, local variations of the thickness. Note also that if we let  $\alpha$  tend to 1, such that  $h_{max} \rightarrow h$ , we obtain the following special case of condition (61)

$$\frac{1}{3(1-\nu^2)} > \frac{1}{g} \tag{63}$$

or

$$\frac{(M_{\xi\xi} - \nu M_{\eta\eta})^2}{(M_{\xi\xi}^2 - 2\nu M_{\xi\xi}M_{\eta\eta} + M_{\eta\eta}^2)} > \frac{2}{3}, \tag{64}$$

which was earlier obtained by Reiss[2] and applied to the minimum compliance design problem for circular plates. Reiss derived condition (64) by considering small, discontinuous variations of the thickness, assuming that the thickness does not vary in the circumferential direction. Within the terminology of the present paper, that is to say that the direction of the stiffeners is fixed.

The solutions  $\alpha$  shown by the solid curve in Fig. 7 are solutions of (61) with the inequality replaced by equality, for  $\nu = 0.25$ . For reasons of completeness, we also show the result for  $\lambda < 1$ , where, however, the stiffeners' directions are to be chosen in the way described earlier. The two dashed lines in Fig. 7 indicate the thickness constraints  $h = h_{max}$  and  $h = h_{min}$ .

The procedure is now as follows. Having obtained a smooth (or partially smooth) design, we on the plate use the thickness  $h$  and the moments obtained, to calculate  $\lambda$  and  $\alpha$  for a selected point. Now, if the point  $(\lambda, \alpha)$  falls within the hatched region of Fig. 7, we can find a suitable  $h_c$  and obtain a negative integrand (55) or (59), and hence reduce the compliance by changing the smooth design locally into the new plate model design. From Fig. 7 we can clearly see that the possibility of smooth designs is restricted to a rather small region for combinations of  $\lambda$  and  $\alpha$ . In particular, we can readily exclude the possibility of smooth designs in the following cases:

$$(1) \quad h_{min} < h < 0.534h_{max}. \tag{65}$$

Notice that condition (65) is only in effect when  $h_{min} < 0.534h_{max}$ .

$$(2) \quad \lambda < 0.6175 \text{ or } \lambda > 1.0/0.6175. \tag{66}$$

Here,  $\nu = 0.25$ .

**Theorem B.** Suppose that there exists a subregion  $\Omega$ , in a smooth, solid plate "optimal"

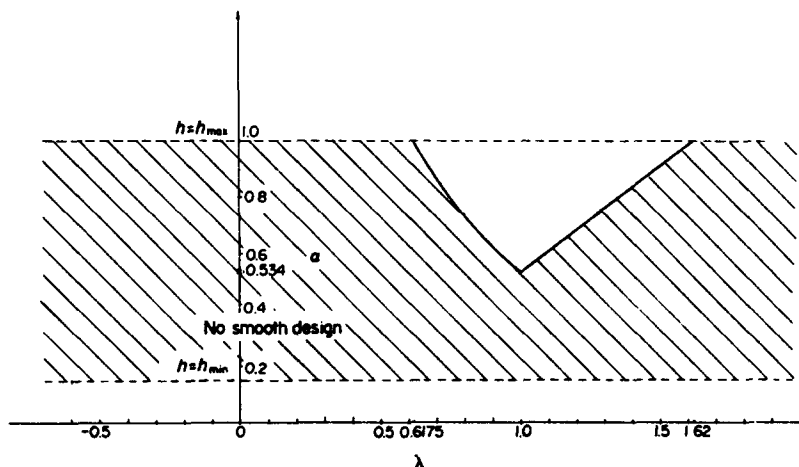


Fig. 7. In the hatched region, smooth design can be improved.  $\alpha = h/h_{max}$ .  $\lambda = M_1/M_2$ ,  $M_1$  and  $M_2$  are the principal moments.

design where

$$h_{\min} < h < h_{\max}, \quad (67)$$

and where

$$\text{the corresponding point } (\lambda, \alpha) \text{ lies in the hatched region of Fig. 7.} \quad (68)$$

The compliance can then be further decreased for unchanged material distribution by constructing in  $\Omega$ , a suitable, generalized new plate model instead of the original smooth one.

As mentioned in the discussion of Theorem A, the conditions in Theorem B are merely sufficient ones. Thus, in a subregion where these conditions are not fulfilled, the new plate model still has the possibility of being superior to the corresponding smooth one. From Theorem B follows a useful corollary:

*Corollary 2.* In any smooth part of a global optimal design of a solid plate, condition (68) must be violated if the thickness  $h$  satisfies

$$h_{\min} < h < h_{\max}.$$

Intuitively, if one obtains a smooth plate design for a large ratio between  $h_{\max}$  and  $h_{\min}$ , there must be a great possibility of finding some subregions where conditions (67), (68) are satisfied. Therefore, an entirely smooth design will hardly be a global optimal one. On the contrary, if the ratio between  $h_{\max}$  and  $h_{\min}$  is small and there are only very small subregions of intermediate thickness in the design, we may not be able to change these subregions into new model plate regions and thereby reduce the compliance.

#### 4. CONCLUSION

In the present paper both analytical and numerical investigations clearly show special features of optimal design problems for solid plates. In general, global optimal solutions of the geometrically constrained, minimum compliance design problem of thin, solid, elastic plates do not exist within the class of continuous functions or continuous functions with a finite number of discontinuities. To determine a possible global optimal design, the design space must therefore be expanded such as to include the class of functions with an infinite number of discontinuities. In this respect, the new formulation developed in this paper should be considered. Similar conclusions [8] are to be expected in the optimization of solid plates with respect to maximizing the fundamental frequency, buckling load, minimizing the largest deflection, etc.

*Acknowledgement*—The author wishes to thank Prof. Frithiof I. Niordson and Niels Olhoff for valuable discussions.

#### REFERENCES

1. K.-T. Cheng and N. Olhoff, An investigation concerning optimal design of solid elastic plates. *Int. J. Solids Structures* (to appear).
2. R. Reiss, Optimal compliance criterion for axisymmetric solid plates. *Int. J. Solids Structures*, 12, 319–329 (1976).
3. H. H. E. Leipholz, Six Lectures on Variational Principles in Structural Engineering, Solid Mechanics Division, University of Waterloo, Waterloo, Ontario, Canada (1978).
4. S. A. Ambartsumjan, *Theory of Anisotropic Plates* (in Russian). Nauka Press, Moscow (1967).
5. S. G. Lekhnitskii, *Anisotropic Plates*. Gordon and Breach Science Publishers, New York (1968).
6. J.-L. Armand, Applications of the theory of optimal control of distributed-parameter systems to structural optimization. NASA, CR-2044 (1972).
7. N. Olhoff, Optimal design of vibrating circular plates. *Int. J. Solids Structures* 6, 139–156 (1970).
8. N. Olhoff, K. A. Lurie, A. V. Cherkav and A. V. Fedorov, Sliding regimes and anisotropy in optimal design of vibrating axisymmetric plates. *Int. J. Solids Structures* (to appear).
9. G. N. Savin and N. P. Fleishman, *Rib-Reinforced Plates and Shells* (in Russian). Naukova Dumka, Kiev (1964).
10. K. A. Lur'e and A. V. Cherkav, Prager theorem application to optimal design of thin plates (in Russian). *MTT (Mechanics of Solids)* 11, 157–159 (1976).
11. K.-T. Cheng, On some new optimal design formulations for plates. Proc. Symp. "Optimization of Distributed Parameter Structures", Iowa City 1980 (Edited by E. J. Haug and J. Cea), Sijthoff and Nordhoff (1981).